AD NUMBER

AD848669

NEW LIMITATION CHANGE

TO

Approved for public release, distribution unlimited

FROM

Distribution authorized to U.S. Gov't. agencies and their contractors; Critical Technology; 14 OCT 1968. Other requests shall be referred to Commanding Officer, Department of the Army, Fort Detrick, Attn: SMUFD-AE-T, Frederick, MD 21701.

AUTHORITY

SMUFD, D/A ltr, 17 Feb 1972

TRANSLATION No. 3341

DATE: 14 Oct 1968

AD848669

DDC AVAILABILITY NOTICE

This document is subject to special export controls and each transmittal to foreign governments or foreign nationals may be made only with prior approval of Commanding Officer, Fort Detrick, ATTN: SMUFD-AE-T, Frederick, Md. 21701

DEPARTMENT OF THE ARMY
Fort Detrick
Frederick, Maryland

37

EFFECT OF THE GEOMETRIC ARC PARAMETERS AND AIR-SOLID MIXTURE CONCENTRATION ON RESISTANCE TO MOVEMENT IN THE BENDS OF LOW PRESSURE PNEUMATIC PIPELINE TRANSPORTERS

Zeszyty Naukowe Politechniki
Lodzkiej, No 79, 1966,
Mechanika, z. 16: 73-106

Marian Markowski,
Lodz Polytechnic Institute
Department of Hoisting
Devices

1. Introduction

Pneumatic pipeline transporters (PPT) are coming into increasingly widespread use for the transport of comminuted materials.

This is due to the following advantages inherent in the method:

- small dimensions;
- ease of adapting a PPT route to the existing local conditions;
- low capital investment outlay;
- ease of pipeline branching or combination of several lines into one;
- no loss of material (apart from the finest fraction lost in the unloading cyclones;
- favorable work safety and hygiene aspect;
- simple supervision and control in view of the small number of moving parts;
- safe means of transporting harmful, noxious and hot materials.

The essential disadvantages of the system are:

- limited application range (low density materials up to 3,200 kg/m^3, in the comminuted state and devoid of stickiness);
- large unit power consumption.

The last disadvantage necessitates research aimed at correct calculation of the magnitude of resistance to motion, definition of the places at which it arises, and explanation of the effect of the major PPT parameters

on the magnitude of these resistances.

The theory of PPT makes use of the general laws of the theory of flow. The following resistances due to friction in straight sections are distinguished:

$$p_t = \lambda \frac{v^2}{2g} \gamma_p \frac{l}{D} \qquad (1)$$

and local resistances

$$p_{sp.m} = \zeta \frac{v^2}{2g} \gamma_p ; \qquad (2)$$

these arise in the vents, T-junctions, the loading and unloading installations, sections of accelerated movement, and places of change in the direction of stream flow. The following designations have been used in the formulas:

λ	coefficient of friction
V (m/sec)	air stream velocity
γ_p (kg/m^3)	density of air for the given atmospheric conditions
L (m)	length of the straight section of pipeline
D (m)	internal diameter of pipe
g (m/sec^2)	acceleration due to gravity
ζ	coefficient of local resistance to flow

In view of considerable repeatibility of direction change places in pipeline systems, and particularly repeatibility of the variously positioned bends, local resistances arising in the bends (hereafter also called arcs) largely affect the total magnitude of resistance offered by a pipeline to the flow of a two-phase system.

According to the data published by the noted expert Prof. Brabbee, the share of all the local resistances in the total resistance of a PPT is as follows:

50 - 150 mm	- 40%
100 - 300 "	- 60"
200 - 600 "	- 80"
400 -1100 "	- 90"
>1100 "	- 95"

The increasing share of the local resistances in the total value with increasing pipeline diameter can be explained by the fact that these resistances (equation 2) are independent of the pipe diameter whereas the resistance due to friction in the straight sections decreases with increasing pipeline diameter (equation 1).

Low-pressure PPT usually have large pipe diameters; hence the

significant share, in the total, of the resistance arising in the bends. This fact underscores the great importance of correct selection of the geometrical parameters of pipeline bends to the efficient functioning of a PPT.

The resistance to motion arising in the course of flow of a mixture of air and the transported material is usually determined on the basis of the relationships true of the flow of pure air, with correction factors introduced to account for the resistance increase due to the introduction of a solid into the air stream.

Accordingly, the static head required to overcome resistance to the flow of an air/solid mixture is defined as

$$p_m = p_p (1 + K\mu), \qquad (3)$$

where: p_m is the static head needed to overcome resistance to the flow of air/solid mixture; p_p is the static head required to overcome resistance to the flow of pure air:

$$p_p = \frac{v^2 \gamma_p}{2g} \left(1 + \lambda \frac{l}{D} + \Sigma \zeta\right), \qquad (4)$$

where: K is the coefficient taking into account the increased resistance due to the presence of solid;

μ is the coefficient of mixture concentration.

In using this formula, the assumption is made that the same value of K is equally true for straight pipeline sections, bends, and other local resistances. However, it is universally held that such an assumption is unfounded and due to the lack of reliable theoretical knowledge and experimental data.

To date, research on PPT has been mainly concentrated on elucidation of the phenomena occuring in the straight sections, a case for which the effect of various factors on the value of K has been studied. However, this research cannot be considered complete. The effect of some factors has not yet been investigated, while the influence of some others has given contradictory or widely divergent results. Therefore, at the moment there is no uniform method for calculation or selection of the value of K for different materials.

Despite great practical significance inherent in the substantial contribution of local resistances (particularly the resistances in bends) to the total value, the amount of attention devoted to the study of K relating to the resistance in bends has been incommensurately small. One encounters in the literature but few attempts at a theoretical approach to the problem. Because of their shortcomings, the relationships proposed

have not found practical application.

The best work to date in this field has been done by G. Weidner /9/. In his theoretical considerations, Weidner took into account the geometric position of an arc (a pipeline bend), and on the basis of an equation of equilibrium of forces acting on material particles moving within the arc, he gave the basic relationships for particle velocity changes and pressure losses due to the arc. However, the simplifying assumptions used by Weidner distort the actual phenomena. These simplifications include neglect of the aerodynamic force acting on particles within the arc, acceptance of the total angle of the arc as the angle at which all the forces act on the particles, and the assumption that the pressure drop for a mixture of air and solid particles flowing through an arc is only slightly greater than that for pure air, and that the total pressure loss occurs beyond the arc. In the available publications, Weidner's work does not include experimental data which might illustrate his theoretical conclusions.

A fuller theoretical picture taking into account all the important forces acting on material particles in their motion within an arc is as follows. The forces acting on a particle moving in an arc are: the centrifugal force, aerodynamic resistance, and the force of gravity with its radial and tangential components. The relative distribution of these forces and their action on the particle depends on the geometric situation of the arc.

We may distinguish five basic positions of an arc: in the horizontal plane (⟶) and four positions in the vertical plane:

1) transition from the horizontal to the vertical direction, upwards motion in the vertical section (⟶↑);

2) transition from the vertical to the horizontal direction, upward motion in the vertical section (↱⟶);

3) transition from the horizontal to the vertical direction, downward motion in the vertical section (⟶↓);

4) transition from the vertical to the horizontal direction, downward motion in the vertical section (↳⟶).

Each of these positions exerts a given effect on the system of forces acting on a particle flowing in an arc, and thereby on the magnitude of velocity and pressure losses.

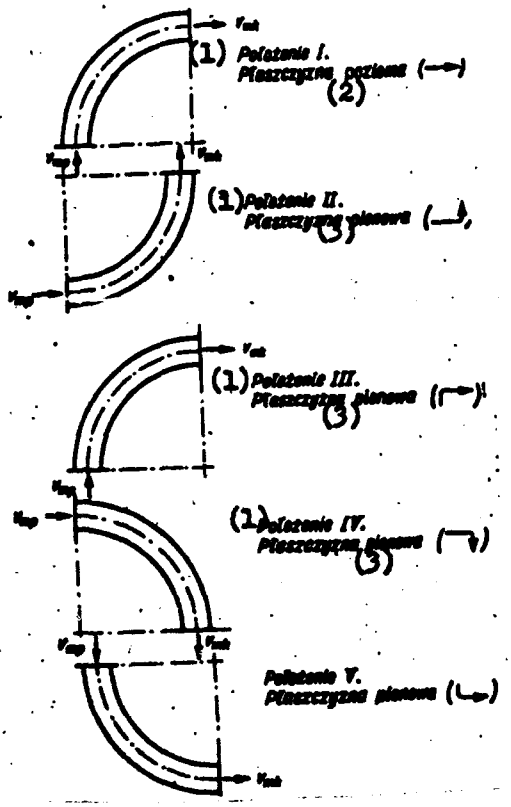

Fig. 1. The five geometric positions of an arc.

/key/: 1. Position; 2. Horizontal plane; 3. Vertical plane.

2. Flow of an Air and Solid Mixture in an Arc

In PPT we deal with a two-phase flow: solid phase (material particles) and gaseous phase (air). The degree of their mutual mixing depends on a number of factors, primarily on the ratio of air velocity to the speed of suspension formation and on the concentration of mixture.

The distribution of material particles through the pipe cross-section depends on the geometric position of the straight section preceeding the arc. In a vertical pipeline this distribution is approximately uniform. In the horizontal sections the distribution depends on the mixture concentration and on the ratio of air velocity to rate of suspension formation. At low concentrations and high V/V_g ratios the material particle distribution through the cross-section may be taken as approximately uniform. As the concentration increases or air velocity decreases (together with the V/V_g ratio), the particle distribution through the cross-section

changes in the direction of increased particle concentration in the lower part of the cross-section and corresponding thinning-out in the upper part. At high concentrations most material particles aggregate in the lower 1/3 of the pipe cross-section /10/. After a given value of the concentration coefficient is attained at a specific value of V/V_z, the heavier particles separate out of the stream and settle on the pipe bottom. The layer thus formed creates increased resistance to flow.

The ratio of the specific gravities of the solid to gaseous components of the mixture is of the order of 600-1,200. This very high ratio of the material to carrier specific gravities is of great importance to the movement of mixture in pipe arcs. High inertia of the transported material in comparison to that of the carrier medium causes the former to preserve the direction of motion it had prior to entering the arc. Change in the direction of particle motion occurs only as a result of the effect of the pipe wall. The motion of particles through an arc is random due to bouncing from the pipe wall and turbulence caused by changes in air velocity along the radius. The cause of this change in velocity distribution lies in the increased concentration of particles near the outer wall and change in the direction of the stream.

The motion of particles through an arc is hindered primarily by friction against the pipe wall and against the particles close to the wall moving at a lower speed. Further slowing down occurs on account of collisions with the wall and with the particles moving more slowly or in the opposite direction. Collisions are more frequent within an arc than in the straight section because of greater concentration of particles and their more random motion.

The material particle and the air streams become intermixed again in the straight section after emergence from a bend, and the particle distribution throughout the cross-section becomes more uniform.

The particles slowed down in the bend become accelerated in the straight section. This acceleration accounts for further loss of pressure in the straight section beyond the bend. Despite the fact that it occurs in the straight section, this pressure drop is caused by the arc, and must be counted among the losses arising in the arc. It is identical with the loss occuring where the material particles become accelerated beyond the loading point, with the difference that acceleration occurs not from zero velocity but from a given velocity V_{mk} attained in the final segment of the arc. This acceleration continues until the particle attains a given constant speed. Beyond the arc, constant speed can be attained in a sufficiently long straight section, and is equal to the constant speed established prior to entry into the arc only in the case of a bend in the horizontal plane. For bends in the vertical position the speed established beyond the arc depends on the actual geometric position of the latter.

3. The Effective Angle of the Arc

The greater inertia of the solid particles in comparison with that of air (the several hundred-fold factor mentioned above) causes the particle trajectories to remain unchanged in the initial segments of the arc, and trajectory curving occurs only after their deflection from the pipe wall. Therefore, the decelerating effect of an arc exists only over a part of its length. This length corresponds to a certain central angle which may be termed the effective angle of the arc. Its value depends on the internal pipe diameter D, the median arc radius R_{gr}, the concentration coefficient, and the geometrical position of the arc. The last two factors determine the position of the gravity center of the mass of material representing the entire mass in the pipe cross-section.

Therefore, the individual geometric positions of the arc must be considered in order to determine the value of the effective arc angle. These considerations will be limited to the central angle of the arc $\delta = 90°$. The value of the effective arc angle for a given geometric position depends on the center of gravity of the mass of material in the pipe cross-section in relation to the axis of this cross-section. For vertical sections of pipeline before a bend, it has been taken that the trajectory of the center of gravity coincides with the symmetry axis of the pipe. On the other hand, in the case of an arc preceeded by a horizontal section the present considerations assume that the center of gravity lies at a height of 1/3D above the pipe bottom. Such an assumption is frequently encountered in the literature, and appears to be reasonable for low-pressure PPT carrying low concentration suspensions.

I. Arc in the horizontal plane.

In accordance with the assumptions, the center of gravity of the mass of material in the pipe cross-section in this case lies 1/3D above the pipe bottom. In addition, the following simplifying assumptions have been made:

1) Particle trajectories prior to encounter with the facing pipe wall are rectilinear (the curved course of the air stream causing the radial exertion of the aerodynamic force on the particles has been ignored);

2) The line of the center of gravity touches the facing (outer) wall of the pipe bend in the plane of an arc passing along the horizontal diameter of the cross-section. The error due to this simplification does not exceed 2% in the most unfavorable case.

Dependence of the effective arc angle on the diameter D and the median radius of arc R_{gr} may be represented as follows (Fig. 2):

$$\sin \alpha = \frac{R_{gr}}{R_{gr} + \frac{D}{2}} = \frac{2 R_{gr}}{2 R_{gr} + D}, \qquad (5)$$

where α is the effective arc angle.

Dividing the numerator and denominator of the above relation by D, we obtain a dependence on the ratio R_{gr}/D:

$$\sin \alpha = \frac{2 \frac{R_{gr}}{D}}{2 \frac{R_{gr}}{D} + 1}. \qquad (6)$$

Applying the above assumptions and simplifications, we can write equations for the value of the effective arc angle for the five cases of geometric arc position given above. The formulas are given in Table 1.

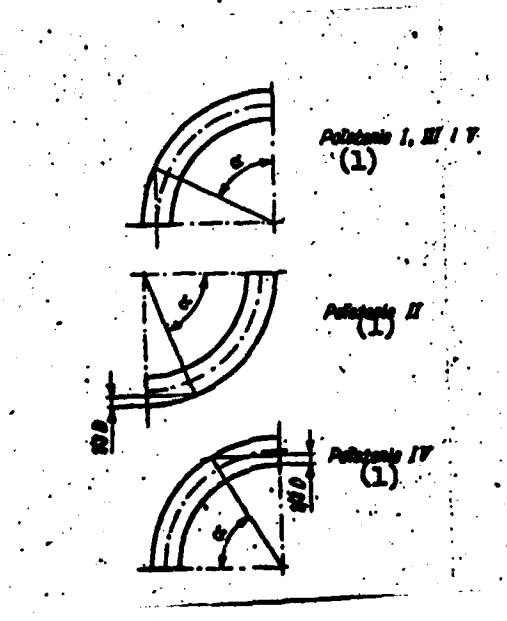

Fig. 2. Diagrams for the calculation of effective arc angles

/Key:/ 1. Position.

The effective arc angle values calculated from these formulas for the five geometric arc positions and for the values R_{gr}/D from 1 to 8 are presented graphically in Fig. 3.

Table 1

Values of the Effective Arc Angles for the Individual Geometric Positions (Central Angle of Arc $\alpha = 90^{\circ}$)

(1) Geometryczne położenie łuku	Wartość czynnego kąta łuku (2)
I Pł. poziom (3) →	$\sin\alpha = \frac{2\frac{R_{gr}}{D}}{2\frac{R_{gr}}{D}+1}$
II Pł. pionowa (4) ↓	$\sin\alpha = \frac{6\frac{R_{gr}}{D}+1}{6\frac{R_{gr}}{D}+3}$
III Pł. pionowa (4) →	$\sin\alpha = \frac{2\frac{R_{gr}}{D}}{2\frac{R_{gr}}{D}+1}$
IV Pł. pionowa ↓ (4)	$\sin\alpha = \frac{6\frac{R_{gr}}{D}-1}{6\frac{R_{gr}}{D}+3}$
V Pł. pionowa (4) ↳	$\sin\alpha = \frac{2\frac{R_{gr}}{D}}{2\frac{R_{gr}}{D}+1}$

/Key/: 1. Geometric position of arc; 2. Value of effective arc angle; 3. Horizontal plane; 4. Vertical plane.

4. Forces Acting on Material Particles Inside a Bend

Assume that in the course of motion through an arc the particle velocity varies from V_{mp} to V_{mk} due to the forces acting on the particles in the course of their flow.

In order to define the relationship between the forces acting on particles within an arc and the changes in their velocity, let us take an infinitely small segment of the arc corresponding to a central angle $d\varepsilon$ and of a length $Rd\varepsilon$. In view of the fact that a preponderant part of the particles is gathered near the outer wall of the bend, in our considerations we must use the outer arc radius R_z and not R_{gr} (Fig. 4). The particle mass m in the segment of arc under consideration is acted upon by the following

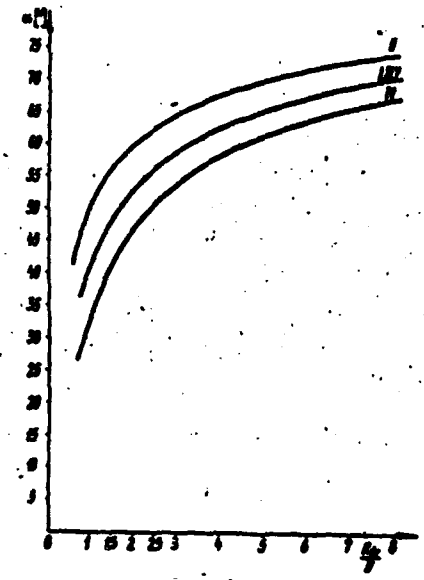

Fig. 3. Dependence of the effective arc angle α on R_{gr}/D for various geometric positions at δ = 90°

forces:

1) centrifugal force $$m \frac{v_m^2}{R} = \frac{\delta_m}{v_m g} R d\varepsilon \frac{v_m^2}{R} \qquad (7)$$

(it is radially directed to the exterior of the bend);

2) the force of gravity

$$mg = \frac{\delta_m}{v_m} R\, d\varepsilon. \qquad (8)$$

This force can be separated into two components: a) the radial component (directed along the arc radius) and the tangential component (perpendicular to the arc radius). The magnitudes of these components depend on the geometric position of the arc and change in the course of motion. The result of the centrifugal force and the radial component of the force of gravity is friction of the material against the bend wall and against particle layers located close to the wall. The direction of friction is always opposite to that of the direction of motion.

Depending on the geometric position of the arc, the tangential component of the force of gravity may either accelerate or retard the particles. In these formulas G_m/kg/sec/ is the amount of material in kg

flowing through the pipeline per second.

3) Aerodynamic resistance force arises as a result of the action of the air stream on the elements within the arc which are either immobile or moving with a velocity lower than that of the air stream. In the case of material particle flow in the arc, aerodynamic resistance depends on the relative velocity, i.e., the difference between air and particle velocities:

$$w = v - v_m. \qquad (9)$$

The value of aerodynamic resistance may be expressed by the equation:

$$W = c \cdot \frac{\pi d^2}{4} \cdot \frac{w^2}{2g} \gamma_p, \qquad (10)$$

where c is the coefficient of aerodynamic resistance.

The value of c varies depending on the shape and the surface state of particles and on the Reynolds number which characterizes flow:

$$c = f(Re), \qquad (11)$$

$$Re = \frac{w d}{\nu}, \qquad (12)$$

where w is the relative particle velocity;
d is the equivalent particle diameter;
ν is the kinematic viscosity coefficient of air.

The value of c may be determined from the approximate formula:

$$c = \frac{a}{Re^2}, \qquad (13)$$

The coefficient a may be taken, with an accuracy sufficient for practical purposes, as a constant value for certain ranges of Re (different for the individual ranges of Re) /9/. In accordance with Newton's second law, we may write for a horizontal pipeline:

$$\frac{a}{Re^2} \cdot \frac{\pi d^2}{4} \cdot \frac{w^2}{2g} \cdot \gamma_p = \frac{\pi d^3}{6g} \cdot \gamma_m \cdot \frac{dv_m}{dt}. \qquad (14)$$

The following relationship holds true for a vertical pipeline:

$$\frac{a}{Re^2} \cdot \frac{\pi d^2}{4} \cdot \frac{w^2}{2g} \cdot \gamma_p = \frac{\pi d^3}{6g} \cdot \gamma_m \cdot \frac{dv_m}{dt} + \frac{\pi d^3}{6} \cdot \gamma_m. \qquad (15)$$

In the course of constant motion, when $dV_m/dt = 0$, the relative velocity is equal to the rate of suspension formation. Of course, this holds true for the vertical sections of a pipeline; on the other hand, it can be accepted as an approximation for the horizontal sections.

For constant motion, relationship (15) may be written in the following form:

$$\frac{a}{Re_z^k} \cdot \frac{\pi d^2}{4} \cdot \frac{v_z^2}{2g} \cdot \gamma_p = \frac{\pi d^3}{6} \cdot \gamma_m \ , \qquad (16)$$

where R_{ez} is the Reynolds number relating to the rate of suspension formation v_z.

On the assumption that in the course of particle velocity changes the relative velocity and the rate of suspension are very close to each other, replacement in (14) of the weight term by the equivalent left side term of (16) and expressing the equation in terms of unit mass gives the following relationship:

$$\frac{1}{g} \cdot \frac{dv_m}{dt} = \frac{Re_z^k}{Re^k} \cdot \frac{w^2}{v_z^2} = \left(\frac{w}{v_z}\right)^{2-k}. \qquad (17)$$

The value of coefficient K depends on the value of Re. For $Re > 1$, i.e., in the region of applicability of square relationship for the calculation of resistances, k = 0; for the region of resistance calculation according to the Stokes relationship ($R_e < 1$), k = 1. In the case of PPT we deal exclusively with turbulent motion, i.e., with the case where $Re > 1$; then k = 0 and equation (17) assumes the form

$$\frac{1}{g} \frac{dv_m}{dt} = \left(\frac{w}{v_z}\right)^2 = \left(\frac{v - v_m}{v_z}\right)^2. \qquad (18)$$

For a material mass present in the element of arc corresponding to the elementary angle $d\varepsilon$, change in movement velocity under the influence of the aerodynamic force is expressed by the equation

$$\frac{\theta_m}{g v_m} R\, d\varepsilon \frac{dv_m}{dt} = \frac{\theta_m}{v_m} R\, d\varepsilon \left(\frac{v - v_m}{v_z}\right)^2. \qquad (19)$$

In the case of a concrete pipeline with given operating conditions and material where V = const and V_z = const, it is seen that the aerodynamic force is a function of the velocity of the material V_m. This is an active force which increases the motion velocity. Friction due to the resultant of the centrifugal force and the radial component of gravity is the passive force retarding motion. Depending on the geometric position of the arc, the tangential compoenent of gravity may be either an active or a passive force, respectively accelerating or retarding particle motion. It is assumed that these are the main forces determining particle velocities and pressure losses. In addition, secondary forces exist whose effect on the motion of material in a pipeline bend is generally small. Among these are inter-particle collisions and stream eddies caused by changes of movement direction in bends.

Changes in particle velocities along an arc are due to the forces enumerated above, and their combination depends on the geometric

position of the arc.

It must be pointed out that in the present considerations it has been assumed that the outer wall of the pipe represents an arc with a radius R, whereas in reality in the case of a circular cross-section the bend consists of cylindrical segments with rectilinear generators. Given a sufficiently large number of segments (according to literature this number is 4-6 for $\delta = 90^\circ$), a bend with a segmented structure can be considered a true arc.

5. Particle Velocity Changes in an Arc

Particle velocity changes under the influence of the forces discussed above should be considered separately for each individual geometric position of the arc.

I. Arc in the horizontal plane.

The following forces act on material particles flowing in an arc in the horizontal position:

1) aerodynamic resistance;
2) centrifugal force;
3) gravity.

Gravity acts in a plane perpendicular to the plane of the arc. The resultant of the centrifugal and gravity forces which generates friction is

$$P = \sqrt{\left(m \frac{v_m^2}{R}\right)^2 + (mg)^2}, \quad (20)$$

and, for an arc element with a length R dε :

$$P' = \sqrt{\left(\frac{G_m}{v_m g} R\, d\varepsilon \frac{v_m^2}{R}\right)^2 + \left(\frac{G_m}{v_m} R\, d\varepsilon\right)^2} = \frac{G_m d\varepsilon}{v_m g} \sqrt{v_m^4 + g^2 R^2}. \quad (21)$$

This resultant force is inclined to the horizontal at an angle γ , which can be determined from the equation

$$\operatorname{tg} \gamma = \frac{mg}{m \frac{v_m^2}{R}} = \frac{gR}{v_m^2}. \quad (22)$$

The resultant force P and its inclination angle γ depend on the outside arc diameter. In an arc situated in the horizontal plane no material is lifted. Therefore, the effect of gravity is expressed only by changes in the magnitude and inclination of the resultant force P. This effect is small. An increase in the resultant force by taking gravity into account would amount to only a few percent in the extreme case. On the other hand, a substantial simplification of the mathematical formulas is achieved by ignoring the effect of gravity. Accordingly, it may be taken that friction in an arc in the horizontal position is due to the centrifugal force only. Therefore,

the force equilibrium equation in this case will have the form:

$$\frac{G_m}{V_m} R\,ds\left(\frac{v-v_m}{v_s}\right)^2 - f\cdot\frac{G_m}{V_m g} R\cdot ds\,\frac{v_m^2}{R} = \frac{G_m}{V_m g} R\,ds\,\frac{dv_m}{dt}\,, \qquad (23)$$

where f is the coefficient of material friction against the pipe wall.

Equation (23) may be transformed to take the form:

$$f\frac{G_m}{V_m g} R\,ds\,\frac{v_m^2}{R} - \frac{G_m}{V_m} R\,ds\left(\frac{v-v_m}{v_s}\right)^2 + \frac{G_m}{V_m g} R\,ds\,\frac{dv_m}{dt} = 0\,, \qquad (24)$$

Dividing this equation by $G_m \cdot R ds$ and multiplying it by $V_m g$, we obtain a differential equation of motion in the form:

$$f\,\frac{v_m^2}{R} - g\left(\frac{v-v_m}{v_s}\right)^2 + \frac{dv_m}{dt} = 0. \qquad (25)$$

In order to eliminate the time differential dt, we can substitute variables on the basis of the relationship:

$$\omega_m = \frac{ds}{dt} \quad i \quad \omega_m = \frac{v_m}{R} \qquad 85a$$

hence

$$dt = \frac{R\,ds}{v_m}. \qquad (26)$$

Substituting this quantity in (25) we obtain

$$f\,\frac{v_m^2}{R} - g\left(\frac{v-v_m}{v_s}\right)^2 + \frac{v_m\,dv_m}{R\,ds} = 0. \qquad (27)$$

After multiplying by R and developing the second term, Eq. (27) will assume the form:

$$v_m\frac{dv_m}{ds} + f\,v_m^2 - \frac{Rg}{v_s^2}\,v^2 + \frac{2Rg}{v_s^2}\,v\,v_m - \frac{Rg}{v_s^2}\,v_m^2 = 0. \qquad (28)$$

Denoting by k the constant quantity for a given arc and material $k = Rg/V_s^2$, we can write

$$v_m\frac{dv_m}{ds} + (f-k)\,v_m^2 + 2k\,v\,v_m - k\,v^2 = 0. \qquad (29)$$

In a concrete case of flow of a constant amount of air given a constant mixture concentration and a pipeline of constant diameter, it can be taken that the mean air velocity V is also constant. In this case, the following designations of constants are introduced to simplify the equation:

$$\begin{aligned} a &= f - k, \\ b &= 2\,k\,v, \\ c &= k\,v^2, \end{aligned} \qquad (30)$$

then the equation of motion can be presented in the form:

$$v_m\frac{dv_m}{ds} + a\,v_m^2 + b\,v_m - c = 0 \qquad (31)$$

or, dividing both sides by V_m:

$$\frac{dv_m}{dz} + a\,v_m + b - \frac{c}{v_m} = 0 \qquad (32)$$

or

$$v'_m = -a\,v_m - b + \frac{c}{v_m}. \qquad (32')$$

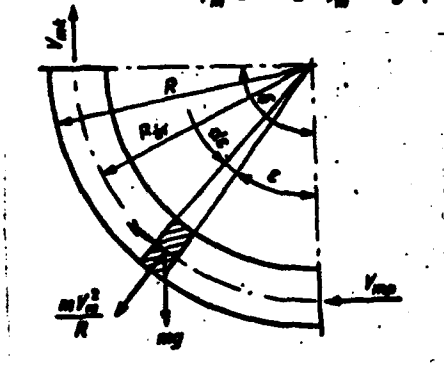

Fig. 4. Forces acting on material particles in a bend

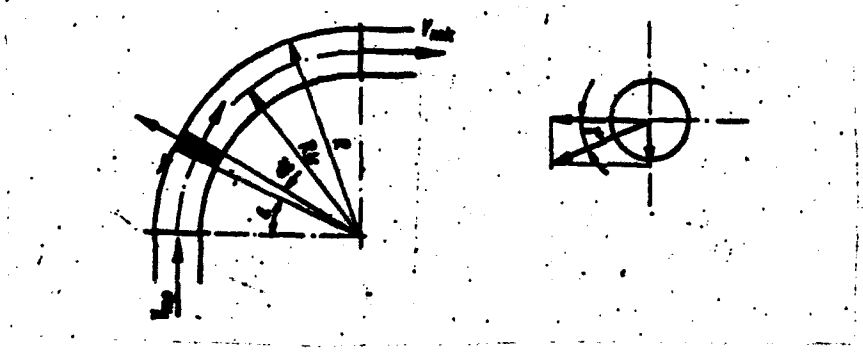

Fig. 5. Schematic of forces acting in the horizontal plane

II. Arc in the vertical position (⟶), transition from the horizontal to the vertical direction, upward motion in the vertical section.

In contrast with the last case, material in this position is lifted to a certain height. The force of gravity lies in the plane of the arc, and directly affects the resultant magnitude of friction. Its effect on velocity changes is substantial.

Preserving the designations of case I, the equilibrium equation can

$$\frac{G_m}{v_m} R\,d\varepsilon \left(\frac{v - v_m}{v_0}\right)^2 -$$

$$- \frac{G_m}{v_m} \cdot R\,d\varepsilon \sin\varepsilon - \left(\frac{G_m}{v_m g} R\,d\varepsilon \frac{v_m^2}{R} +\right.$$

be written as follows:

$$\left. + \frac{G_m}{v_m} R\,d\varepsilon \cos\varepsilon\right) \cdot f = \frac{G_m}{v_m g} R\,d\varepsilon \frac{dv_m}{dt}. \tag{33}$$

Applying the transformations and substitutions as before, we obtain

$$v_m \frac{dv_m}{d\varepsilon} + (f - k) v_m^2 + 2k v' v_m - k v^2 + \tag{34}$$

Substituting

$$a = f - k,$$
$$b = 2k v,$$
$$c = k v^2,$$
$$d = f Rg,$$
$$e = Rg,$$

$$+ f Rg \cos\varepsilon + Rg \sin\varepsilon = 0. \tag{35}$$

we obtain the final differential equation of motion in the form:

$$v_m \frac{dv_m}{d\varepsilon} + a v_m^2 - b v_m - c + \frac{d}{v_m} \cos\varepsilon + \frac{e}{v_m} \sin\varepsilon = 0, \tag{36}$$

and, dividing the sides by V_m, we have

$$\frac{dv_m}{d\varepsilon} + a v_m + b - \frac{c}{v_m} + \frac{d}{v_m} \cos\varepsilon + \frac{e}{v_m} \sin\varepsilon = 0 \tag{36'}$$

or

$$v_m' = - a v_m - b + \frac{c}{v_m} - \frac{d}{v_m} \cos\varepsilon - \frac{e}{v_m} \sin\varepsilon = 0. \tag{36''}$$

In a similar manner we obtain the differential equations of motion for the remaining three geometric positions of the arc in the vertical plane. These equations are compiled in Table 2.

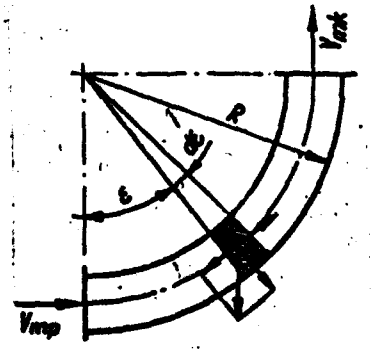

Fig. 6. Schematic of forces acting in the vertical plane in position II (⟶)

Table 2

Differential Equations of Motion of Particles in an Arc Conduit

Geometryczne położenia łuku (1)	Symbol (2)	(3) Różniczkowe równanie ruchu
I Pł. (4) poziома	→	$v_m' = -av_m - b + \frac{c}{v_m}$
II Pł. pionowa (5)	↑	$v_m' = -av_m - b + \frac{c}{v_m} - \frac{d}{v_m}\cos\varepsilon - \frac{e}{v_m}\sin\varepsilon$
III Pł. pionowa (5)	↱	$v_m' = -av_m - b + \frac{c}{v_m} + \frac{d}{v_m}\sin\varepsilon - \frac{e}{v_m}\cos\varepsilon$ wzór słuszny dla zakresu (6) $\frac{v_m^2}{R} > g\sin\varepsilon$
IV. Pł. pionowa (5)	↳	$v_m' = -av_m - b + \frac{c}{v_m} + \frac{d}{v_m}\cos\varepsilon + \frac{e}{v_m}\sin\varepsilon$ (6) wzór słuszny dla zakresu $\frac{v_m^2}{R} > g\cos\varepsilon$
V Pł. (5) pionowa	↳	$v_m' = -av_m - b + \frac{c}{v_m} - \frac{d}{v_m}\sin\varepsilon + \frac{e}{v_m}\cos\varepsilon$

/Key/: 1. Geometric position of arc; 2. Symbol; 3. Differential equation of motion; 4. Horizontal plane; 5. Vertical plane; 6. Equation holds for the range.

The conditions (Table 2) at which the equations for positions III and IV are true limit their applicability to the case of particle motion along the outer wall of the pipe bend. When the inequality is fulfilled in the direction opposite to that given in Table 2, the particles would be pressed against the inner wall of the arc by a force given by the difference between the radial component of gravity and the centrifugal force. In that case the equation should contain the value of the internal arc radius, and the sequence of the terms in the bracket multiplied by the friction coefficient f should be changed. It may also happen (V_m decreases along the arc, and the value of the sin function increases) that particles will travel along the outer wall for some distance and along the inner wall subsequently, in which case the above two types of equation would hold true. It should be pointed out that reverse eddies close to the inner wall, especially near the end of the arc, radically alter the nature of the phenomenon and make its mathematical representation impossible.

Most frequently encountered in practice is the case considered above, i.e., (88a) $\frac{v_m^2}{R} > g\sin\varepsilon$ or (88b) $\frac{v_m^2}{R} > g\cos\varepsilon$. The reasons why it

is considered typical are readily apparent. A confirmation of this will be furnished by the following numerical example:

If $V_m = 5$ m/sec and R = 2.5 m, then $V_m^2/R = 10$, which is greater than the value of g sinε for the terminal point of the arc (always $\varepsilon < \delta = 90^\circ$). It should be stressed that the employed value of R = 2.5 is very large and rarely encountered in concrete PPT, whereas $V_m = 5$ m/sec is rather small.

The differential equations of particle motion in an arc are the Abel equations of the second kind of the general form:

$$[y + g(x)]\, y' = f_2(x)\, y^2 + f_1(x)\, y + f_0(x). \qquad (37)$$

This form is in accordance with the original version given in the work "Ouvres Completes de H.N. Abel", Vol 2.

In the case under consideration

88c

$$\begin{aligned} y &= v_m, \\ x &= \varepsilon, \\ g(x) &= 0, \\ f_2(x) &= -a, \\ f_1(x) &= -b, \\ f_0(x) &= c \pm d\begin{Bmatrix}\cos\varepsilon \\ \sin\varepsilon\end{Bmatrix} \pm e\begin{Bmatrix}\sin\varepsilon \\ \cos\varepsilon\end{Bmatrix}. \end{aligned}$$

In the general case this equation has no integral solution. There are particular solutions for the cases $f_1(x) = 0$ or $f_0(x) = 0$. Thus the equations of particle motion in an arc given in Table 2 cannot be presented in the integral form. They have, therefore, been solved approximately by the Heming method using a ZAM-2β computer. In this manner tables of approximate solutions have been obtained. These tables were used to construct graphs of particle velocity changes in bends of various R_{gr}/D ratios ranging from 1 to 8, using characteristic numerical data for two materials: wheat and beechwood chips.

The values of 10 and 15 m/sec have been used as the initial velocities in constructing the graphs illustrating material particle velocity changes in arcs having various R_{gr}/D ratios. In these graphs the values of effective arc angle have been marked for each R_{gr}/D value. Also constructed were graphs illustrating the particle velocity changes corresponding to the theoretical equations not taking into account the effect of the aerodynamic force on the particles within the volume of the pipe bend (i.e., the equations derived by Weidner). This makes possible to separate the pressure losses caused by the arc into the part occuring within the arc itself and the part manifesting itself in the straight portion of pipe beyond the bend.

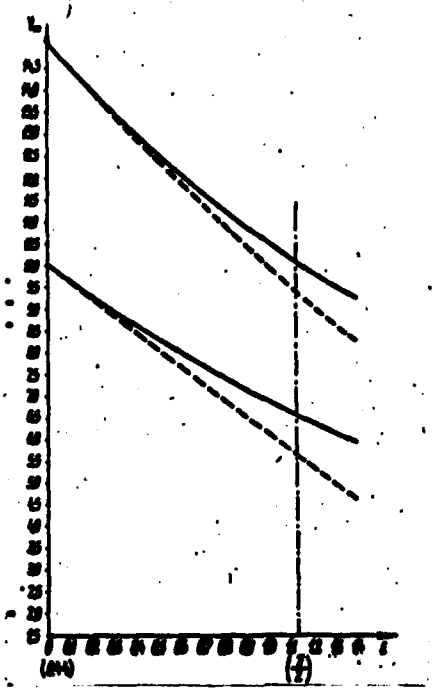

Fig. 7. Graph of Particle velocity changes in an arc in the horizontal position (II: ⟶) with $R_{gr}/D = 3$. Materail: wheat.

Figure 7 shows, as an example, one of the graphs of particle velocity changes within a bend.

For each geometric position of the arc, collective graphs have been constructed illustrating the dependence of particle velocity loss ΔV_m within an arc on the outer arc radius or, in tne case of constant diameter, on the values of R_{gr}/D. Examples of these graphs are given in Figs. 8-12. In these graphs are plotted the total particle velocity loss V_{mc}, as well as the partial loss sustained within the arc itself ΔV_{gt} and in the straight section beyond the arc ΔV_m pr. Pressure losses due to the arc and occuring in the arc itself and in the straight section beyond are proportional to the corresponding values of ΔV_{mt} and ΔV_m pr.

6. Pressure Loss Coefficients in the Art

The problem of particle velocity changes occuring in an arc and the need to accelerate them in the bend itself and in the straight section is associated with a loss of pressure expended to achieve this acceleration. This loss may be calculated on the basis of the impulse principle:

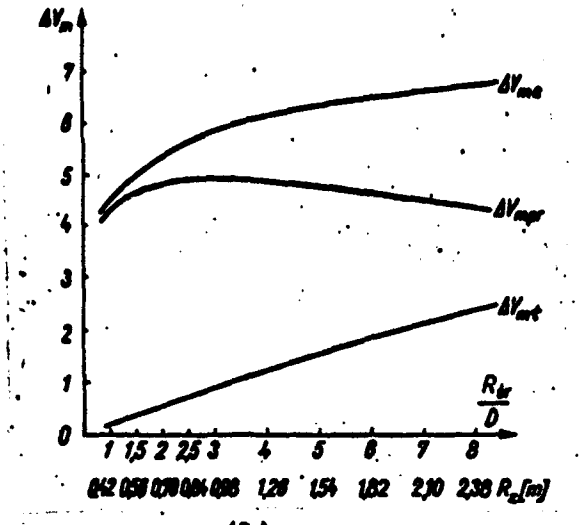

Fig. 8 Variation of 90a $\Delta V_m = f\left(\frac{R_{kr}}{D}\right)$ and $f(R_z)$ for an arc in the horizontal plane; position 1; material: beechwood chips, V_{mp} = 15 m/sec.

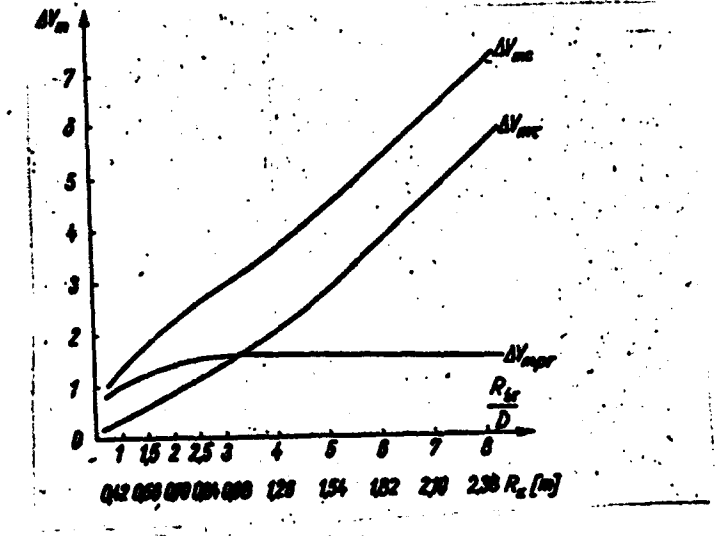

Fig. 9. Collective graph of 90b $\Delta V_m = f\left(\frac{R_{kr}}{D}\right)$ and $f(R_z)$ for an arc in the vertical position; position II (⟶); material: beechwood chips, V_{mp} = 10 m/sec.

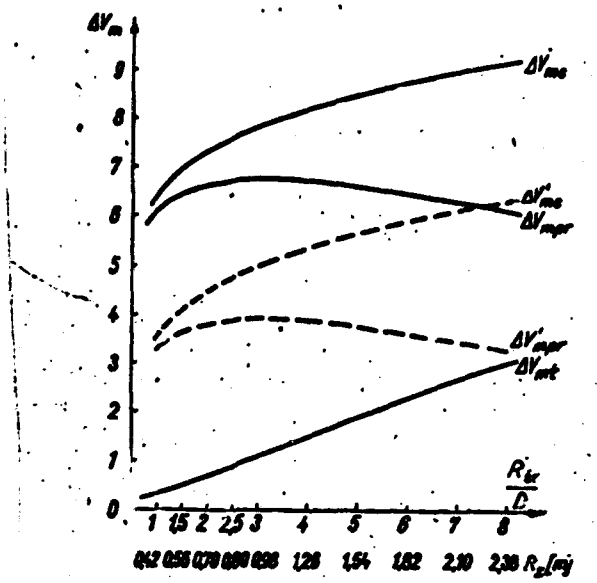

Fig. 10. Collective graph of 91a $\Delta V_m = f\left(\frac{R_{tr}}{D}\right)$ vs $f(R_g)$ for an arc in the vertical plane; position III ( ), material; wheat, V_{mp} = 15 m/sec.

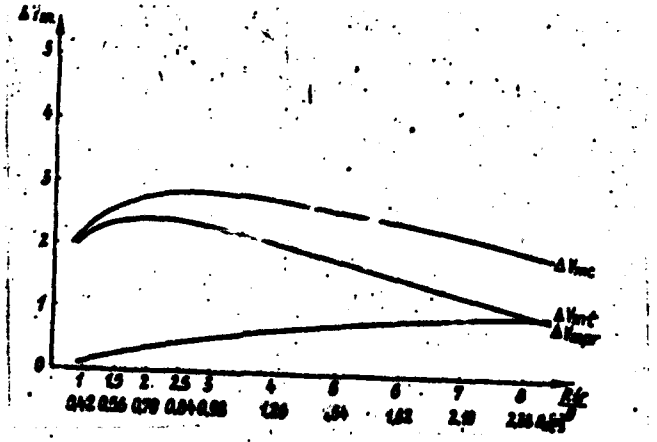

Fig. 11. Collective graph of 91b $\Delta V_m = f\left(\frac{R_{tr}}{D}\right)$ vs $f(R_g)$ for an arc in the vertical plane; position IV ( ), material: beechwood chips, V_{mp} = 10 m/sec.

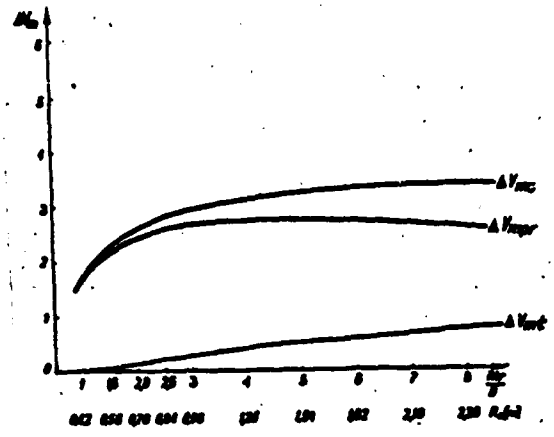

Fig. 12. Collective graph of 92a $\Delta V_m = f\left(\frac{R_z}{D}\right)$ vs $f(R_z)$ for an arc in the vertical plane (↪); material: beechwood chips, $V_{mp} = 15$ m/sec.

$$\Delta p_t = \frac{\gamma_p \mu V}{g} \Delta V_m \quad [kG/m^2], \tag{38}$$

where Δp_t - loss caused by the arc;

γ_p - density of air;

V - average air velocity;
μ - weight concentration coefficient of mixture;
$\Delta V_m = V_{mp} - V_{mk}$ - change of particle velocity within the arc.

As we know, the total pressure loss due to the arc is divided in two parts, according to the place of occurrence associated with the resumption of the velocity lost in the arc:

1) with an effective angle in the arc itself: Δp_{t1};
2) in the straight section beyond the arc: Δp_{t2}

$$\Delta p_t = \Delta p_{t1} + \Delta p_{t2}, \tag{39}$$
$$\Delta V_m = \Delta V_{m1} + \Delta V_{m2}.$$

Both these values can be calculated from equation (38):

$$\Delta p_{t1} = \frac{\gamma_p \mu V}{g} \Delta V_{m1}, \tag{38'}$$
$$\Delta p_{t2} = \frac{\gamma_p \mu V}{g} \Delta V_{m2}. \tag{38''}$$

The quantity ΔV_{mt} to be substituted in Eq. (38') consists of the value corresponding to the section of the vertical straight line which, in the graph, denotes the effective angle of the arc subtended between the curves of particle velocity changes in the arc plotted, respectively, from the formulas including and neglecting the effect of the aerodynamic force on the particles. The quantity $\Delta V_{m\,pr}$ substituted in (38") consists of the difference between the steady velocity attained by the particles beyond the arc and that which the particles travel in the outlet cross-section of the bend, i.e., the value (read for the effective angle of the arc) from the graph of velocity change whithin the arc which takes into account the effect of the aerodynamic force.

This procedure for an arc in the horizontal position is illustrated in Fig. 13 which represents the course of $V_m = f(\varepsilon)$.

The value of the steady velocity attained by the particles past the bend depends on the geometric position of the arc:

1) In the case of position I (in the horizontal plane) the steady velocity beyond the arc may be equal to that established before the arc. In this case the equation for calculating the pressure loss due to an arc should include the velocity difference between the values before the arc (V_{mp}) and at the end of it (V_{mk}), which represents the pressure loss due to the arc:

$$\Delta V_{m\,pr} = V_{mp} - V_{mk} \tag{40}$$

2) Position II (the vertical plane ↑). Here the material velocity may attain the maximum value $V'_m = V - V_g$ when before the arc the velocity $V_{mp} = \varphi V$ had a different (generally greater) value. Then

$$\Delta V_{m\,pr} = (V - V_g) - V_{mk}\,; \tag{41}$$

where

$$\varphi = \frac{V_g}{V}\,.$$

93a

3) Position III (the vertical plane: →). The particle velocity before the bend may have the value $V_{mp} = V - V_g$, whereas beyond the arc the steady velocity attained may be $V'_m = \varphi V$, generally higher than the value before the arc (the bend is followed by a horizontal section of pipe).

The acceptance of the theoretically valid principle that the difference between the initial velocity before the bend and the velocity attained by the particles in its outlet cross-section is to be taken as the maximum velocity loss due to an arc logically results in the need for additional acceleration of particles beyond the bend from $V_m = V - V_g$ to $V'_m = \varphi V$.

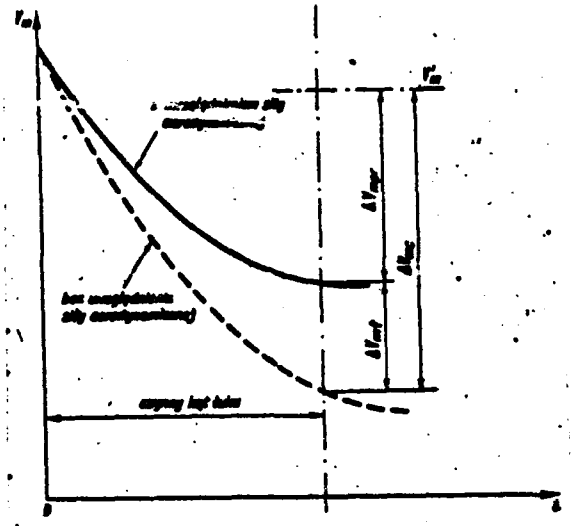

Fig. 13. Schematic for calculation of particle velocity losses in an arc.

/Key/: 1) Including the aerodynamic force; 2) Neglecting the aerodynamic force; 3) Effective arc angle.

Therefore, it appears advisable to include this additional difference in the total velocity loss due to an arc. Then the velocity loss used in the equation for pressure loss calculations will increase by $V_z - (1-\varphi)V$ and will be $V_{m\,pr} = \varphi V - v_{mk}$.

4) Position IV (in the vertical plane: ⟶↓). Depending on the downward length of the straight section, the particle velocity attained beyond the bend may be greater than before it. This is caused by the combined action, within the bend, of the tangential component of gravity and the aerodynamic force. Beyond the bend the whole force of gravity is active, and it combines its action with that of the aerodynamic force until the particle velocity equals that of the air stream. Later, at $V_m > V$, the aerodynamic force begins to hinder the motion of particles, which may attain a velocity $V_m = V + V_z$. Only the pressure expenditure required to propel the particles to the velocity V_{mp} which they had before entering the arc should be considered as pressure loss due to the arc and manifesting itself in the straight section beyond the arc.

$$94a \qquad \Delta v_{mpr} = \varphi \cdot v - v_{mk}.$$

5)Position V (in the vertical plane: ↳). The particle velocity before the arc depends on the length of the corresponding straight section of the pipeline and may be greater than that of the air stream. The particle velocity in the horizontal section beyond the arc may attain the value $V_m' = \varphi V$ (smaller than the air stream velocity). In this case the pressure

loss due to the arc depends on the particle velocity in the initial cross-section of the effective part of the arc, and in the particular case may equal zero.

The same particle velocities (10 and 15 m/sec) were used in plotting the graphs, whereas the air stream velocities V used depended on the geometric position of the arc.

For positions I, II and IV, $V = V_m \varphi$; for position III (⌐→), $V = V_m + V_z$, and for position V (↪), $V = V_m$.

The foregoing reasoning makes it possible to derive theoretical formulas defining the coefficient of resistance to the motion of an air/material mixture in an arc ζ_{tm} or the coefficient K_t which takes into account the effect of the material on the increase of flow resistance of a mixture in relation to the resistance to the flow of pure air in accordance with Eq. (3).

Considering the equation for resistance in an arc arising in the course of material transport

$$\Delta p_m = \zeta_{tm} \cdot \frac{v^2}{2g} \gamma_p , \tag{42}$$

we can write

$$\zeta_{tm} = \frac{2g}{v^2} \frac{\Delta p_m}{\gamma_p} . \tag{43}$$

Adopting the commonly used formula which takes into account the increased resistance due to the flow of material particles, we can write

$$\Delta p_m = \zeta_{tp} \frac{v^2}{2g} \gamma_p (1 + K_t \mu), \tag{44}$$

while referring to Eq. (42):

$$\zeta_{tm} = \zeta_{tp} (1 + K_t \mu). \tag{45}$$

This relationship enables us to determine the coefficient K_t

$$K_t = \frac{\frac{\zeta_{tm}}{\zeta_{tp}} - 1}{\mu} . \tag{46}$$

At the same time, taking into account the total pressure loss in an arc (i.e., the loss due to the flow of pure air plus the additional expenditure needed to accelerate the material particles), we can write

$$\Delta p_m = \zeta_{tp} \frac{v^2}{2g} \gamma_p + \frac{\gamma_p \mu v}{g} \Delta v_m = \frac{v^2}{2g} \gamma_p \left(\zeta_{tp} + \frac{2\mu}{v} \Delta v_m \right). \tag{47}$$

Substituting this value in (43) we obtain

$$\zeta_{tm} = \zeta_{tp} + \frac{2\mu}{\nu} \Delta v_m , \qquad (48)$$

in turn, this quantity substituted in (46) gives

$$K_t = \frac{2}{\nu} \frac{\Delta v_m}{\zeta_{tp}} . \qquad (49)$$

It follows from the last two equations that both the value of the resistance coefficient ζ_{tm} and the coefficient K_t at a constant air speed depend on particle velocity changes in the arc and on the experimentally determined coefficient of resistance to the flow of pure air in an arc ζ_{tp}. Indirectly, both these coefficients are a function of the outer arc diameter (or the ratio R_{sr}/D at a constant value of D). They also depend on the physical characteristics of the material being transported, i.e., the coeffient of friction and the speed of suspension formation.

Theoretical calculation of the material particle velocity changes in an arc will always suffer from some error for the following reasons:

1) A real material always consists not of selected uniform and identical particles but rather of a mixture of particles differing in weight, size and shape for which the rates of suspension formation will be different, whereas the equations for computation of the aerodynamic force contain a uniform value which is, as a rule, true for the largest and heaviest particles.

2) Eddies of both air and material particles exist in a bend, and there is interaction between particles. The equation does not take these effects into consideration; it only takes into account the effect of the major and most important forces, although the influence of the neglected secondary forces is obvious. At any rate these phenomena are not amenable to theoretical manipulation if only because they are random, irregular and dependent on a number of peripheral causes.

The proper numerical values of the resistances and coefficients comprising summarily all the losses occuring in an arc can only be obtained experimentally. The aim of such an experiment should be to confirm the correctness of the theoretical considerations, to establish the discrepancy between the calculated and experimental values and to gather experimental data required for determining the coefficients needed in practical applications.

7. Experimental Investigation of Pressure Losses in the Bends of Low Pressure PPT During Material Transport

In order to verify the theoretical solutions presented above, tests were run on an experimental installation, comprising measurement of pressure

losses occuring during the transport of an air /material mixture. Pressure were measured in the bend (Δp_{mt}) and in the straight section beyond ($\Delta p_{m.r}$).

7.1. Test Stand

The test stand consisted of a low pressure PPT of the ram type comprising a pipe with an internal diameter D = 280 mm and straight section lengths of about 56 m, and 11 bends changing the direction of flow. Variable-radius elbows (constant diameter D, variable R_{sr}/D ratio) were used where the changes in flow direction occured in the horizontal plane and in the vertical plane in position II (—↑) (transition from the horizontal to the vertical direction, upward motion in the vertical section). A study was made of the effect of the value of outer arc radius and the R_{sr}/D ratio on the pressure drop caused by an arc in six pipe bends having the following R_{sr}/D values: 1.5, 2.0, 2.5, 3.0, 4.0 and 6.0. The quantity of the solid material fed was varied in order to investigate the effect of the concentration factor on flow resistance. The following material flow rates were used in the study:

wheat: G = 0 7, 1.0, 1.2 and 1.5 kg/sec;
beechwood chips: G = 0.35, 0.5, 0.6 and 0.7 kg/sec.

A fan with an output of about 7,000 m^3/hr and a static pressure of about 400 mm water column was used to generate an air stream. The material to be transported was introduced into the stream through a loading device located just beyond the fan. Two types of loading device were used: the shelf type and the drum type. The unloading was done in a cyclone located at the end of the pipeline. The material separated from the air stream was collected in the bottom part of the cyclone and was allowed to drop into a container. A weighing - metering device was used to feed strictly defined amounts of material into the system. The device consisted of two belt conveyors: the upper one (constituting the bottom of a container) functioned as a metering device collecting the desired amounts of material from the container, while the lower one weighted the amount of material dispensed.

8. Measurements and Measuring Instruments

The following quantities were measured on the test stand:

1) the amount of material introduced into the pipeline;
2) the static pressure distribution in the pipeline;
3) the total and dynamic pressure distribution through the pipe cross-section.

8.1. Measurement of Material Quantity

Measurement of the amount of material introduced into the stream per unit time was intended to determine the mixture concentration. The

quantity of material was measured with the aid of a clockwork sensor having a 0.01 mm division scale. The basis of measurement was the bending of a flat spring bearing on one end the frame of the weighing conveyor suspended on a knife edge. The regulated length of the spring made it possible to align the number of sensor divisions with the quantity of material dispensed in unit time. Calibration of the scale (i.e., determination of the number of sensor divisions corresponding to 1 kg/sec of material) was accomplished by weighing portions of material delivered over a given period of time.

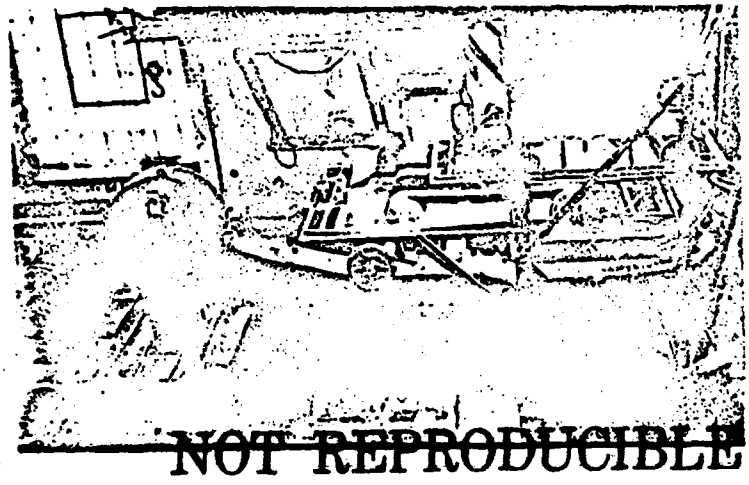

Fig. 14. General view of test stand

8.2. Measurement of Static Pressure Distribution in the Pipeline

Holes were drilled in the pipe at characteristic points where pressure measurements had to be made. The hole edges were smoothed, and short lengths of pipe were welded on for connection to a battery manometer by means of rubber tubing. Static pressure was measured in the initial and final cross-sections of bends in the horizontal position, those situated in the vertical position (position II : ⟶), and at points 18 m beyond the bend in the straight portion of pipe situated in the horizontal position. In the straight section the measurement points were located every two meters. No measurements were done in the remaining three positions of the arc (III - V). The pressure drop over a section of pipe is obtained as the difference between the pressure values at the beginning and the end of a given section.

8.3. Measurement of Pressure Distribution Through Pipe Cross-Section

The aim of this measurement was to determine the distribution of air velocities in the pipe cross-section, calculate the average velocity and, in effect, to determine the air output per second. Knowing the air output and the amount of material introduced per unit time, it was possible

to calculate the weight concentration factor of the mixture. Measurements were done at nine points of pipe cross-section: at the two extremes located at 4 mm from the pipe wall, and seven in intermediate locations at equal intervals from each other. Static and total pressure was measured at these points, the difference of these two values giving the dynamic pressure. The pressure distribution in the pipe cross-section was measured using the Prandtl hook sensors. These sensors could not be used for pressure measurement in the course of material mixture flow since their orifices soon became clogged by the dust accompanying the movement of material particles. This purpose was achieved by using straight sensors inserted at 45° in the direction of flow. Such sensors gave rather considerable pressure indication error. To eliminate this error, all the sensors were calibrated in a calibration tunnel. In processing experimental data, corrections were introduced using the calibration results in the form of graphs. The short pipe stubs and sensor terminals were connected by rubber tubing with the terminals of a 22-tube battery manometer on which the pressure values for the individual measurement points were read off. For better visibility, the manometer tubes were frequently filled with colored denatured alcohol. The height of the individual manometer columns was recorded by photographing the battery manometer face. The results were read off the films using a readout device and recorded in tables. The photographic technique enabled simultaneous recording of pressure at all measurement points and performance of many measurements at approximately the same atmospheric conditions and a similar state of the transported material. To eliminate the momentary variations present in turbulent motion, each measurement was repeated from several to over ten times, and average values were used in subsequent calculations.

9. Results of Measurements

The pressure value for each individual measurement point consisted of the difference between the liquid colum heigth in the tube connected to the atmosphere and that connected to a given measurement point as read off the photographic film. The results in terms of the spirit column heigth were re-calculated into water column heigth values, taking into account the temperature at which the measurement was made. The results were reduced to a constant value of air density so that measurements made under different atmospheric conditions could be compared. The value of the specific gravity of air $\gamma = 1.2$ kg/m^3 was used as the reference value. The conversion was made according to the Boyle-Mariotte equation

(50)

where: p_1 is the reduced pressure corresponding to specific gravity of air $\gamma_1 = 1.2$ kg/m^3;
p_2 is the pressure under given atmospheric conditions (the sum of the static and atmospheric pressures in the pipeline;
γ_2 is the specific gravity of air corresponding to given atmospheric

pressure p_2;
$\gamma_1 = 1.2$ kg/m^3.

The difference between the static pressures measured at the beginning and the end of a bend gave the pressure loss sustained in that bend. The pressure along the straight section beyond the bend was measured to determine the additional pressure loss due to the bend but manifesting itself in the straight section. This loss, incurred to accelerate material particles, is calculated from the static pressure changes along the straight section. For this purpose it was necessary to plot a pressure drop graph for the straight section. The length of the straight section was plotted on the abscissa in a suitable scale, marking the positions of the individual measurement points, while the pressure measured at these points was plotted on the ordinate. The pressure in the final segment of the bend was used as the reference pressure (equal to zero). The line joining the points so plotted is a curve for a section immediately following the bend, and becomes a straight line further on. The straight portion corresponds to the section of steady motion, while the curve corresponds to acceleration, i.e., occurence of a further pressure loss. Extrapolation of the straight line portion corresponding to pressure changes along the straight pipe to the point of intersection with the ordinate denotes the point on the latter whose value is equal to the amount of pressure lost in the straight section of the pipe beyond the bend. This is illustrated in Fig. 15.

As before, the total pressure (the sum of the static and dynamic pressures) and the static pressure readings obtained from pressure distribution measurements in the pipe cross-section were converted to the water column equivalents and reduced to the pressure corresponding to $\gamma = 1.2$ kg/m^3. The difference of these two pressures represents the reduced dynamic pressure. The air stream velocity was calculated for each measurement point in the pipe cross-section from the value of dynamic pressure using the equation

$$v = \sqrt{\frac{2g \cdot p_d}{\gamma_p}} \text{ [m/sek] (51)} \qquad (51)$$

The distribution of air velocity vectors in the pipe cross-section forms a flattened paraboloid of revolution with the axis coinciding with that of the pipe. This paraboloid may be deformed by stream turbulence caused, among others, by the assymetric distribution of material in the cross-section and by other obstacles.

Having the flat distribution of the velocities measured along the cross-section diameter (velocity distribution was measured only in the plane of the bend), we can calculate the volume of the paraboloid which will be equal to the output of air per second:

$$Q = 2\pi \int_0^R v\, r\, dr \quad \text{[m}^3\text{/sek]}. \qquad (52)$$

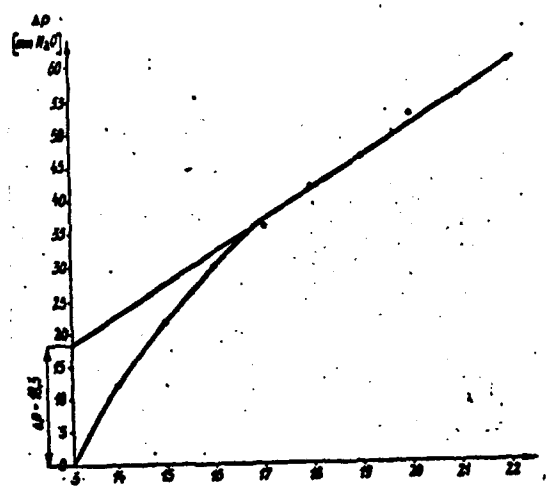

Fig. 15. Schematic for calculation of additional pressure loss in the straight section beyond bend.

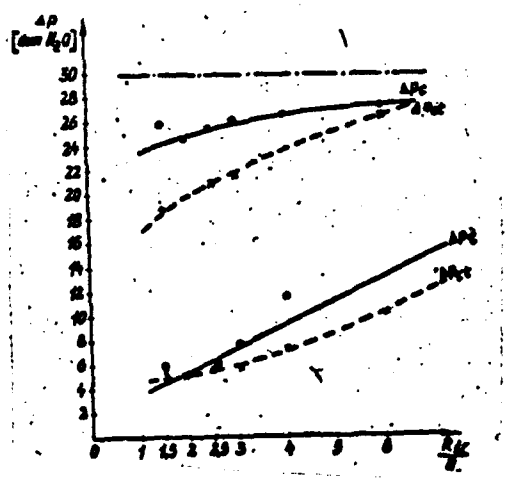

Fig. 16. Graph of pressure loss due to an arc in the horizontal position; material: wheat, G = 1.2 kg/sec.

and the weight output per second

$$G_p = Q \cdot \gamma_p = 2\pi \gamma_p \int_0^R v\, r dr \quad [kG/sek]. \qquad (53)$$

The average air velocity for the cross-section can be obtained by dividing the volume yield by the pipe cross-section area:

$$v_{av} = \frac{Q}{F} = \frac{2\pi \int_0^R v\, r dr}{\frac{\pi D^2}{4}} = \frac{8 \int_0^R v\, r dr}{D^2} \quad [m/sek]. \qquad (54)$$

Knowing the amount of material G_m (in kg/sec) introduced into the stream and the weight flow rate of air G_p (in kg/sec), we can determine the weight concentration coefficient for the mixture

$$\mu = \frac{G_m}{G_p}. \qquad (55)$$

After processing, the measurement results were displayed in the form of the following graphs:

1) graphs of pressure loss due to an arc in the horizontal position as a function of the outer arc radius (and R_{sr}/D), containing pressure change curves which take into account the losses in the straight section beyond the bend (the total loss): 101a $\Delta p_t^I = f(R)$ and R_{sr}/D; and the pressure change curves for the bend: 101b $\Delta p_t^I = f(R)$ and (R_{sr}/D);

2) graphs of pressure drop in an arc situated in the vertical position II (⟶↑) as a function of the outer arc radius (and R_{sr}/D): 101c $\Delta p_t^{II} = f(R)$ and R_{sr}/D);

3) graphs of K_t^I coefficients as a function of the mixture concentration coefficients 101d $K_t^I = f(R)$ and 101e $K_t^I = f(\mu)$;

4) graphs for 101f $K_{t1}^I = f(R)$ and (R_{sr}/D) and 101g $K_{t1}^I = f(\mu)$;

5) graphs for 101h $\left(\frac{R_{kr}}{\Lambda}\right)$ and (R_{sr}/D), and 101i $K_{t1}^I = f(\mu)$

The following notation has been used:

K_t^I is a coefficient taking into account the effect of material on the increase in the total resistance to motion for an arc situated in the horizontal plane;

K_{t1}^I is the coefficient taking into account the effect of material on the increased resistance to motion within an arc situated in the horizontal position;

K_{t1}^{II} is the coefficient taking into account the effect of material on resistance increase in an arc situated in the vertical position II (⟶↑).

The graphs selected as an illustration are shown in Figs. 16-23.

In order to compare the results of measurements with theoretical calculations, it is necessary to have for the latter the data corresponding to the same starting conditions as those employed in the experiment. To this end, the experimentally determined air velocity in the pipeline and the calcu-

lated initial velocity of the material have been used in the theoretical formulas. The results obtained from calculations using these data are plotted in the graphs as a dotted line.

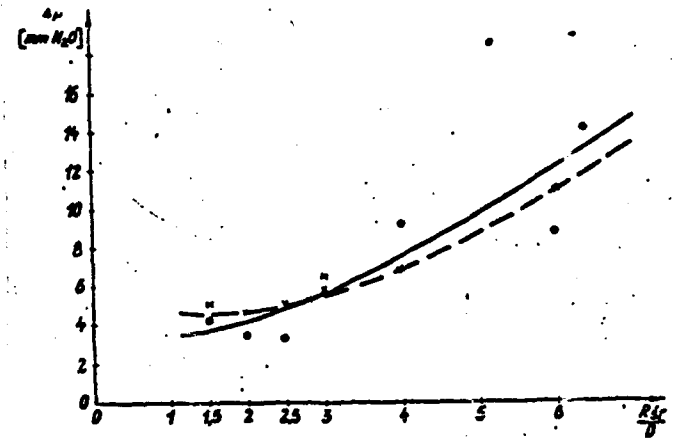

Fig. 17. Graph of pressure loss within a bend in the vertical plane. Material: beechwood chips, G = 0.6 kg/sec.

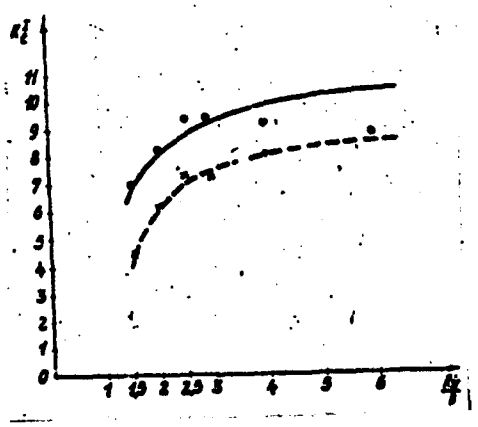

Fig. 18. Graph of $\frac{\Delta p}{\gamma}$ 102a for wheat. G = 1.2 hg/sec.

An analysis and comparison of the experimental results with the theoretical considerations and calculations lead to the following conclusions:

1. The procedure hitherto employed for calculation of resistance in pipeline bends and based on the acceptance of the coefficient K (which takes into account the effect of material on flow resistance increase) at a value identical with that for the straight sections is unjustified. The values of K for bends are considerably higher than those for straight sections.

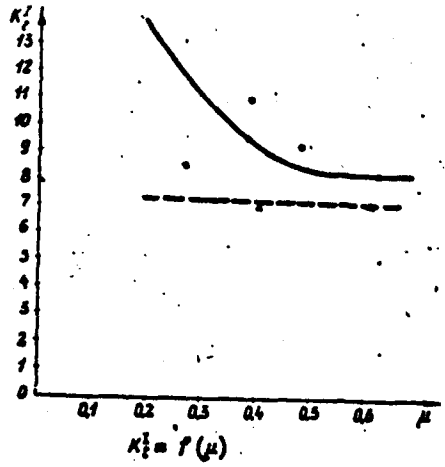

Fig. 19. Graph of 103a for wheat. $R_{sr}/D = 3$.

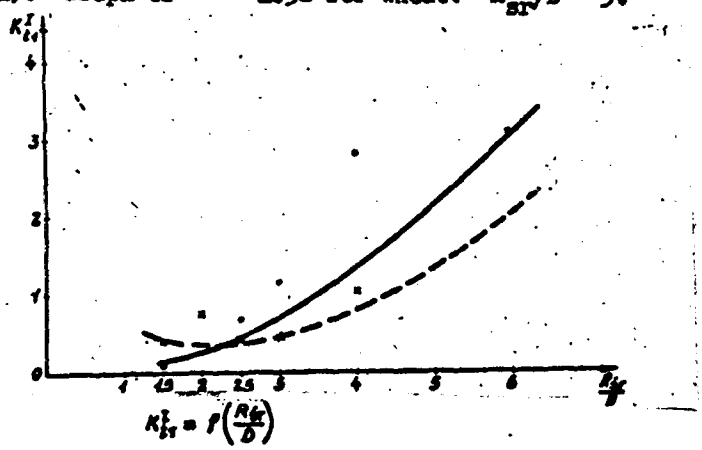

Fig. 20. Graph of 103b for wheat. G = 1.2 kg/sec.

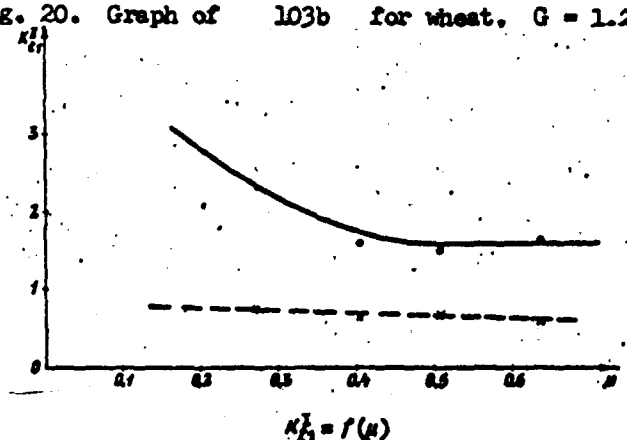

Fig. 21. Graph of 104a for wheat. $R_{sr}/D = 3$.

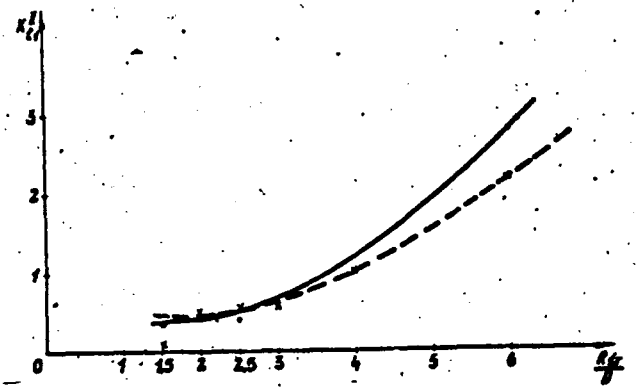

$K^{II}_{L1} = f\left(\frac{\bar{R}_{sr}}{D}\right)$

Fig. 22. Graph of 104b for wheat. G = 1.2 kg/sec.

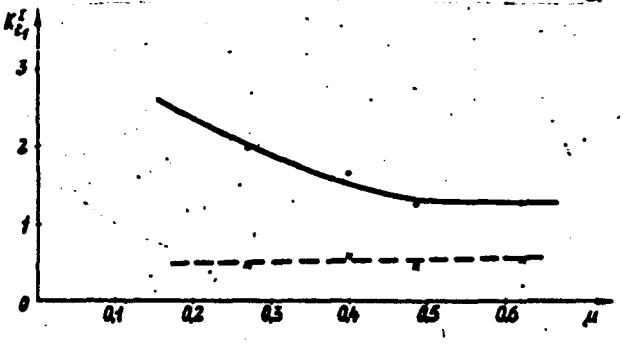

Rys. 23. Wykres wartości $K^{II}_{L1} = f(\mu)$ dla pszenicy; $\frac{R_{sr}}{D} = 3$

Fig. 23. Graph of 105a for wheat. $R_{sr}/D = 3$.

Furthermore, Weidner's approach cannot be considered satisfactory because of the simplyfying assumptions he adopted. Among others, his approach does not provide the means for dividing the pressure losses into the parts arising in a bend and in the straight section beyond. This may lead to wrong conclusions concerning the value of the resistance coefficient obtained from experimental measurements.

2. The adequate agreement between the experimental and theoretical curves makes it possible to believe that the model of the forces acting on particles within an arc as presented above is satisfactory, and that the main forces determining the magnitude of losses due to bends have been taken into account. The existing discrepancies can be explained by the fact that the additional secondary influences discussed above, changes in the physical characteristics of materials in the course of measurements and measurement errors have been ignored in the present considerations.

3. The magnitude of resistance due to a bend depends on its geometric position and on the value of the outside arc radius (at a constant value of R_{sr}/D). This statement is an additional argument against the correctness of the old method for calculating resistances in pipeline bends using K values true of the straight pipe sections.

4. For bends situated in the horizontal plane. lower values of R_{sr}/D and the outside arc radius are more advantageous.

5. This principle is still more strongly applicable to positions II (⤴) and III (↪) than to the case of the horizontal position. In the case of positions IV and V (⤵ and ↳ respectively), bends with higher values of R_{sr}/D are more advantageous for low initial particle velocities.

6. The use of arcs with low R_{sr}/D values (1.5, 2.0) is not recommended, since then the effect of the ignored factors becomes fairly substantial and divergence from theory quite large. It seems that arcs with R_{sr}/D = 2.5; 3.0 are the most advantageous.

7. The coefficient of friction of the material against the the pipe wall is the quantity determining the magnitude of resistance in bends.

8. Further experimental investigation, especially at medium and high pressures, is needed to confirm that the thesis presented above is valid for the entire range of pressures employed in PPT.

BIBLIOGRAPHY

[1] J. G a s t e r s t ä d t: Die experimentelle Untersuchung des pneumatischen Fördervorgange.

[2] K.R. K a r g: Pneumatische Materialtransporte unter besonderer Berücksichtigung des Späneabsaugs-anlagen.

[3] K.J. S t r a c h o v i c z: Osnovy tieorii i rasczieta pnievmaticzeskich transportnych ustanovok.

[4] A.B. L v o v i c z: Pnievmaticzeskij transport na tiekstilnych predprijatiach.

[5] W.A. U s p i e ń s k i: Pnievmaticzeskij transport.

[6] A.M. D z i a d z i o: Pnievmaticzeskij transport na ziernopierorabatyvajuszczich predprijatiach.

[7] M.Ch. D o r f m a n: Pnievmaticzeskij transport zierna i produktov jego pierierabotki.

[8] M. K a l i n u s z k i, Z.Z. O r ł o v s k i j, J.S.S i e g e l: Pnievmaticzeskij transport v stroitielstvie.

[9] G. W e i d n e r: Grundsätzliche Untersuchungen über den pneumatischen Fördervorgang insbesondere über die Verhaltnisse bei Beschleunigung und Umlenkung. "Forschung auf dem Gebite des Ingenieurwesens", Nr. 21, 1955.

[10] G. W e L s c h o f: Pneumatische Förderung bei grossen Fördergutkonzentrationen, VDI - Forschungsheft Nr 492, 1962.